SCIENCE CHINA
Technological Sciences

•Article•

April 2023 Vol.66 No.4: 1129–1140
https://doi.org/10.1007/s11431-022-2178-8

The drug loading behavior of PAMAM dendrimer: Insights from experimental and simulation study

ZHOU LiPing[1,2,3†], LI JiaWei[4†], YU Bing[1,2], ZHANG Jun[4*], HU Hao[1*], CONG HaiLin[1,2*] & SHEN YouQing[1,5]

[1] *Institute of Biomedical Materials and Engineering, College of Materials Science and Engineering, Qingdao University, Qingdao 266071, China;*
[2] *State Key Laboratory of Bio-Fibers and Eco-Textiles, Qingdao University, Qingdao 266071, China;*
[3] *Beijing Key Laboratory for Bioengineering and Sensing Technology, School of Chemistry and Biological Engineering, University of Science and Technology Beijing, Beijing 100083, China;*
[4] *School of Materials Science and Engineering, China University of Petroleum, Qingdao 266580, China;*
[5] *Center for Bionanoengineering and Key Laboratory of Biomass Chemical Engineering of Ministry of Education, College of Chemical and Biological Engineering, Zhejiang University, Hangzhou 310027, China*

Received June 7, 2022; accepted August 10, 2022; published online March 13, 2023

Poly(amidoamine) (PAMAM) dendrimers are widely studied as drug vectors due to their particular structure and excellent properties. Drug molecules can be loaded in the internal cavity of dendrimers or adsorbed on the surface. In this paper, the interaction force and spatial configuration between PAMAM and several typical chemotherapy drugs (doxorubicin (DOX), paclitaxel (TAX), hydroxycamptothecin (HCPT)) is studied by molecular dynamics (MD) simulations. Several essential parameters of dendrimers as drug carriers are analyzed by combining experiments and MD simulations, including particle size, drug loading, drug release, and biocompatibility. The simulation of dendrimer@drug complexes demonstrates that many cavities are semi-open, and most drug molecules are not completely wrapped. The internal structure of PAMAM dendrimers became looser with more extended nuclei, which increased the non-covalent interactions between PAMAM dendrimers and drug molecules. The umbrella sampling simulations reveal that the change of binding energies between dendrimers and drug molecules is responsible for the variation in drug release rate. This study provides valuable enlightenment information for the drug loading/release of PAMAM dendrimers.

PAMAM, dendrimer, chemotherapy, molecular dynamics simulation, binding energies

Citation: Zhou L P, Li J W, Yu B, et al. The drug loading behavior of PAMAM dendrimer: Insights from experimental and simulation study. Sci China Tech Sci, 2023, 66: 1129–1140, https://doi.org/10.1007/s11431-022-2178-8

1 Introduction

Dendrimers are a kind of macromolecule material composed of central nuclei, repeating units, and terminal groups [1,2]. Poly(amidoamine) (PAMAM) dendrimers are macromolecules with well-defined, nanosized, and highly branched monodispersed structures [3]. High-generation dendrimers have a center-symmetric three-dimensional (3D) structure, which is approximately spherical. Dendrimers have the characteristics of adjustable size, shape, surface group, and internal void space, making them widely used in drug delivery, gene therapy, and biosensing [4–7].

Many drug molecules are hydrophobic and can be easily removed by kidneys and phagocytes when injected directly.

†These authors contributed equally to this work.
*Corresponding authors (email: zhangjun.upc@gmail.com; huhao@qdu.edu.cn; hailincong@yahoo.com)

Therefore, drug delivery systems are necessary to help drug molecules reach the lesion site efficiently [8,9]. The drug delivery systems based on dendrimers exhibit good properties in efficiently delivering chemotherapeutic drugs. The dendrimer-based carriers enable hydrophobic chemotherapeutics to achieve solubilization, prolong the circulation time *in vivo*, accumulate in the lesion site, and penetrate into the tumor [10,11]. As shown in Figure 1, loaded cargoes can be encapsulated in the internal cavity of the dendrimer, or they can be attached to the macromolecule's surface through electrostatic or covalent interaction [12]. Dendrimers' generation and peripheral groups are closely related to cargo loading and release. High-generation dendrimers usually have high drug loading due to more extensive and internal cavities; the abundant active groups on the surface provide convenience for modifications, such as targeting [13,14].

Although dendrimers have been widely studied as drug carriers, there is no detailed theoretical support for the relationship between macromolecules and drug molecules. When researchers explain the drug-loading behavior of dendrimer carriers, they usually use experimental results to speculate and explain experimental phenomena, which lack theoretical support [15,16]. With advanced computer technology and simulation methods, dendrimers' interaction and spatial configuration at the atomic and molecular levels can be intuitively explained by utilizing molecular dynamics (MD) simulations. The mainstream MD method, including all-atom MD simulation and coarse-grained MD simulation, provides a supplementary approach for researching dendrimer-loaded drugs [17,18]. Utilizing molecular simulation, researchers established more detailed knowledge regarding the effect of pH values, generations, counterions, and surface modification on load/release properties of dendrimers [19–21], as well as the interactions between dendrimers and cell membranes [22]. For example, using atomistic MD simulations, Maingi et al. [23] have analyzed the release pattern of four ligands (salicylic acid, *L*-alanine, phenylbutazone, and primidone), which were initially encapsulated inside the PAMAM dendrimer using the docking method. Jain et al. used Nateglinide (antidiabetic, belongs to Biopharmaceutics Classification System class II) as a model drug to assess the structural properties such as radius of gyration, shape, radial density distribution and solvent accessible surface area of dendrimer-drug complexes through MD simulations [24]. However, most current related research is either only experiments or theoretical analysis. The investigations of load/release properties of dendrimers by combining experiments and simulations are scarce.

In this work, we used different aliphatic amines (ethylenediamine (EDA), 1,4-diaminobutane (DAB), 1,6-diaminohexane (HMD), and 1,8-diaminooctane (OMDA)) and methyl acrylate (MA) as monomer pairs to prepare PAMAM dendrimers with different cavity sizes and a different number of surface functional groups. With combined MD simulations and experimental results, we explored the relationship between dendrimers and three model chemotherapy drugs (doxorubicin (DOX), paclitaxel (TAX), hydroxycamptothecin (HCPT)). The results confirmed that dendrimers prepared using long-chain fatty amine units have larger internal cavities. These dendrimers possess a loose and uniform structure, which is favorable for the encapsulation of drug molecules. The drug-release profiles demonstrate that both the generation and molecular structure determine the drug-releasing performance. The release rate of high-generation dendrimers in a neutral environment is lower than that of low-generation dendrimers. The umbrella sampling simulations suggest that the change of binding energies between dendrimers and drug molecules is responsible for the variation in drug release rate. The cytotoxicity of different dendrimers and dendrimer-drug complexes was evaluated.

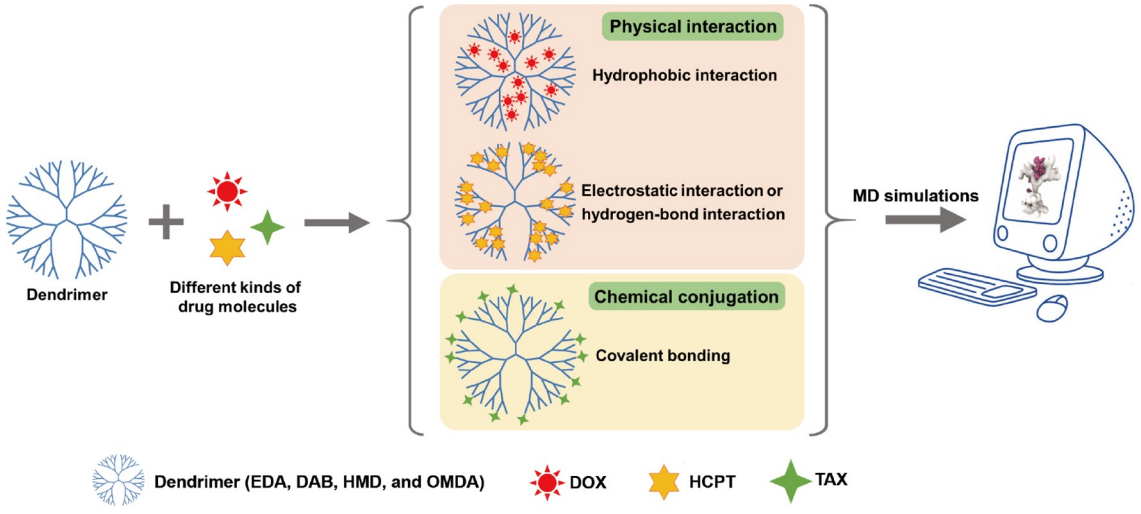

Figure 1 (Color online) Schematic diagram illustrating the possible relationship between PAMAM dendrimers and drugs.

According to MD simulations, the changing trend of cell viability was analyzed. This article revealed the interaction mechanism between drug molecules and dendrimers, which provides theoretical support for researching dendrimer-based drug carriers.

2 Experimental section

2.1 Chemicals

Ethylenediamine (EDA, 99.5%), 1,4-diaminobutane (DAB, 99.5%), 1,6-diaminohexane (HMD, 99.5%), 1,8-diaminooctane (OMDA, 99.5%), methyl acrylate (MA, 99.0%), doxorubicin hydrochloride (DOX, 98%), paclitaxel (TAX, 99%), and (S)-10-hydroxycamptothecin (HCPT, 98%) were obtained from Aladdin Chemistry Co. Ltd. (Shanghai, China). All chemicals were used without further purification.

2.2 Material preparation

2.2.1 Preparation of dendrimers

As reported before, dendrimers were synthesized using MA and EDA [3]. Briefly, aliphatic amine was added to 25 mL of methanol, and then MA was added dropwise into the solution under a nitrogen atmosphere. The reaction was stirred at 4°C for 30 min and an additional 24 h at room temperature. Methanol and excess MA was evaporated off using a rotary evaporator. Then the half-generation (G0.5) PAMAM dendrimer was obtained. To prepare the G1 PAMAM, a certain amount of aliphatic amine was added dropwise to 25 mL of G0.5 PAMAM dendrimer solution in methanol under a nitrogen atmosphere. The reaction was stirred at 4°C for 30 min, then at room temperature for 24 h. G1 PAMAM was obtained after removing methanol and excess aliphatic amine by using a rotary evaporator at 55°C. The steps for synthesizing high-generation dendrimers are similar. For dendrimers prepared from DAB, HMD, and OMDA, the crude product was precipitated by hexane or ice ether after being evaporated [3]. The detailed experimental procedures to prepare PAMAM dendrimers are shown in the Supporting Information.

2.2.2 Characterization of the dendrimers

The composition of dendrimers was examined by Fourier transform infrared spectroscopy (FTIR, Nicolet AVATAR-360, Thermo Scientific, USA). A drop of dendrimer solution was added to the sample stage. FTIR spectra were recorded in transmission mode. The particle size of the dendrimers was measured using the Zetasizer Nano-ZS instrument (ZEN3700, Malvern Instruments Limited, UK). PAMMA dendrimers were dissolved in methanol solution with different concentrations for DLS.

2.2.3 Drugs loading and releasing in vitro

A typical procedure for the preparation of drug-loaded PAMAM complexes (PAMAM@drug) in an aqueous solution by a dialysis method was as follows. 100 mg of PAMAM dendrimers were dissolved in 20 mL of methanol separately. 20 mg of the model drug (DOX, TAX, or HCPT) was added to the above solutions, and the solutions were stirred for 48 h at room temperature. The resultant systems were dialyzed against water to remove the free drugs. The model drugs' loading amount was analyzed by testing the drug concentration in the solution after dialysis using a UV-vis spectrophotometer (UH4150, Hitachi High-Tech Science Corporation, Tokyo, Japan) at a determined absorbance wavelength (DOX at 470 nm, TAX at 234 nm and HCPT at 360 nm). The loading capacity (LC) was calculated by

$$\mathrm{LC} = \frac{M_1}{M_0 - M_1} \times 100\%, \tag{1}$$

where M_0 is the mass of the dendrimer, and M_1 is the mass of the drug loaded into the dendrimer.

For drug release assay, 1 mL of PAMAM@drug solution in PBS (0.01 mol L^{-1}, pH 7.4) was enclosed in the dialysis bag. The dialysis bag was immersed in 10 mL of PBS at 37°C. At predetermined time points, 1 mL of the medium solution was taken away, and 1 mL of fresh PBS was added back. The amounts of released drugs were evaluated by the UV-vis spectrophotometer. All of the release tests were carried out in triplicate. The percentage accumulative release (%) of model drugs was calculated by

$$\text{Accumulative release (\%)} = \frac{\text{Accumulative release drug amount}}{\text{Total drug amount}} \times 100\%. \tag{2}$$

The cumulative amounts of released drugs were calculated from a standard calibration curve (Figure S1, Supporting Information).

2.3 *In vitro* cytotoxicity assay

The cytotoxicity of the dendrimers was analyzed by MTT assay in the NIH 3T3 and HepG2 cell lines. The NIH 3T3 and HepG2 cell lines were acquired from the Cell Bank of Shanghai, Chinese Academy of Sciences (Shanghai, China). The cells were seeded in a 96-well microplate at 10^4 cells/well density and incubated in 100 μL of DMEM/well for 24 h. The culture medium was replaced with a fresh medium containing dendrimers or kinds of dendrimer@drug at various concentrations, and the cells were incubated for 24 h. Then, 10 μL of MTT reagent (5 mg/mL) was added to each well. After 4 h, the medium was removed by aspiration, and 100 μL of DMSO was added to each well. The absorbance at 570 nm was measured using a microplate reader (Model 680, BIO-RAD, USA). Detailed procedures were described previously [25].

3 Molecular dynamics simulations

All-atom molecular dynamics simulations were utilized to capture the structural information of PAMAM dendrimers and as well as to investigate the interactions between dendrimers and drug molecules. The widely used OPLS-AA force field was applied to simulate the interaction among PAMAM dendrimers, methanol solution, and drug molecules [26]. Parameters for molecules were generated using TPPmktop. Nose-Hoover thermostat algorithm and Parrinello-Rahman algorithm were chosen to control temperature and pressure, respectively. The non-bonded potential truncation was performed with a cut-off radius of 1.2 nm for the Lennard-Jones potential, and the long-range electrostatic interactions were treated with the particle mesh Ewald (PME) method. In this study, all simulations were carried out at a pressure of 1 bar and a temperature of 298 K with a coupling constant of 0.1 ps. The widely used Maxwell-Boltzmann distribution sets the initial atomic velocities of systems, the simulation box is periodic in all three directions, and the time step of simulations was 1 fs. The molecular dynamics simulations were performed in GROMACS 5.0.4 software package [27]. Visual Molecular Dynamics (VMD) software was used to visualize the simulation results.

3.1 Simulation process

The initial configurations of the simulation were built by the software package Packmol [28]. In the study of the structural properties of dendrimers, each simulation system contains one dendrimer molecule, which was placed in the center of the simulation box. In the study of the interaction between dendrimers and drugs, the simulations started from randomly dispersed one dendrimer molecule and twenty drug molecules. The steepest descent method was applied for energy minimization. After minimization, 20 ns MD simulation in the isothermal-isobaric (NPT) ensemble was carried out to achieve an equilibrium state. The last 2 ns of MD simulation in equilibrium was used to collect data for analysis. Moreover, the density and potential energy of simulation systems as well as the radius of gyration and the root-mean-square deviation of dendrimers were analyzed to ensure rationality and accuracy of simulations, as shown in Figure S2.

3.2 Umbrella sampling

The umbrella sampling method was used to analyze the binding energy between PAMAM dendrimers and drug molecules [29]. To compute the potential of mean force (PMF) profile of the target molecules (PAMAM@DOX, PAMAM@TAX and PAMAM@HCPT) versus the center-of-mass (COM) distance, the stable dendrimer@drug complexes were placed in a new rectangular simulation box which contains methanol solution. After energy minimization and MD simulation in the NPT ensemble, the COM of selected drug molecule was pulled along the given reaction coordinate while PAMAM dendrimer was restrained. Based on the configurations obtained from the trajectory, a series of separate simulations were run along the reaction coordinate, biased by umbrella potentials. Afterward, the PMF profiles were obtained using the Weighted Histogram Analysis Method [30] implemented in the GROMACS simulation package. The process of umbrella sampling simulation was examined to ensure its adequacy and accuracy of umbrella sampling simulation.

4 Results and discussion

4.1 Synthesis and characterization of the PAMAM dendrimers

A series of PAMAM dendrimers were synthesized successfully by MA and kinds of aliphatic amines (EDA, DAB, HMD, and OMDA), named PAMAM(EDA), PAMAM (DAB), PAMAM(HMD) and PAMAM(OMDA) respectively. The typical FTIR and ^{1}H NMR spectra of PAMAM dendrimers are shown in Figures S3 and S4. The PAMAM dendrimers display the characteristic -NH_2 stretch at 3250 cm^{-1}. In the FTIR spectra, the peaks at 3250 cm^{-1} for -N-H- stretching vibrations and 1630–1562 cm^{-1} correspond to the deformation vibration of the amide Ⅱ band. The disappearance of -$COOCH_3$ absorption peaks indicates that the entire generation of dendrimers was successfully synthesized. In ^{1}H NMR spectra, when the aliphatic amine/MA ratio is 12:1, the peak at δ = 3.23 ppm disappears, which means the formation of a perfect dendrimer with amino groups all over the surface [3]. The peak located at the chemical shift of δ = 1.25 ppm is attributable to the inner methylidyne protons between the oxygen moieties. FTIR and ^{1}H NMR spectra confirmed the successful preparation of PAMAM dendrimers.

For dendrimers, the size of the particle reflects the internal cavity and directly affects the LC. The particle size of dendrimers was measured by dynamic light scattering (DLS). In MD simulations, the theoretical particle size of PAMAM is gained by averaging the length of PAMAM (the minimum energy state) in the *x*/*y*/*z*-direction. As shown in Figure 2(a), with the increase of the generation in dendrimers and as the carbon chain gets longer, the particle size of the dendrimer measured by DLS increased from 3.12 nm (G3 PAMAM (EDA)) to 13.5 nm (G5 PAMAM(OMDA)). All experimental values are larger than the simulated theoretical values. The difference is more obvious in the high-generation groups. This phenomenon may be caused by the DLS test principle, which measures the hydrodynamic diameter of particles. Simulation only describes the ideal situation. Be-

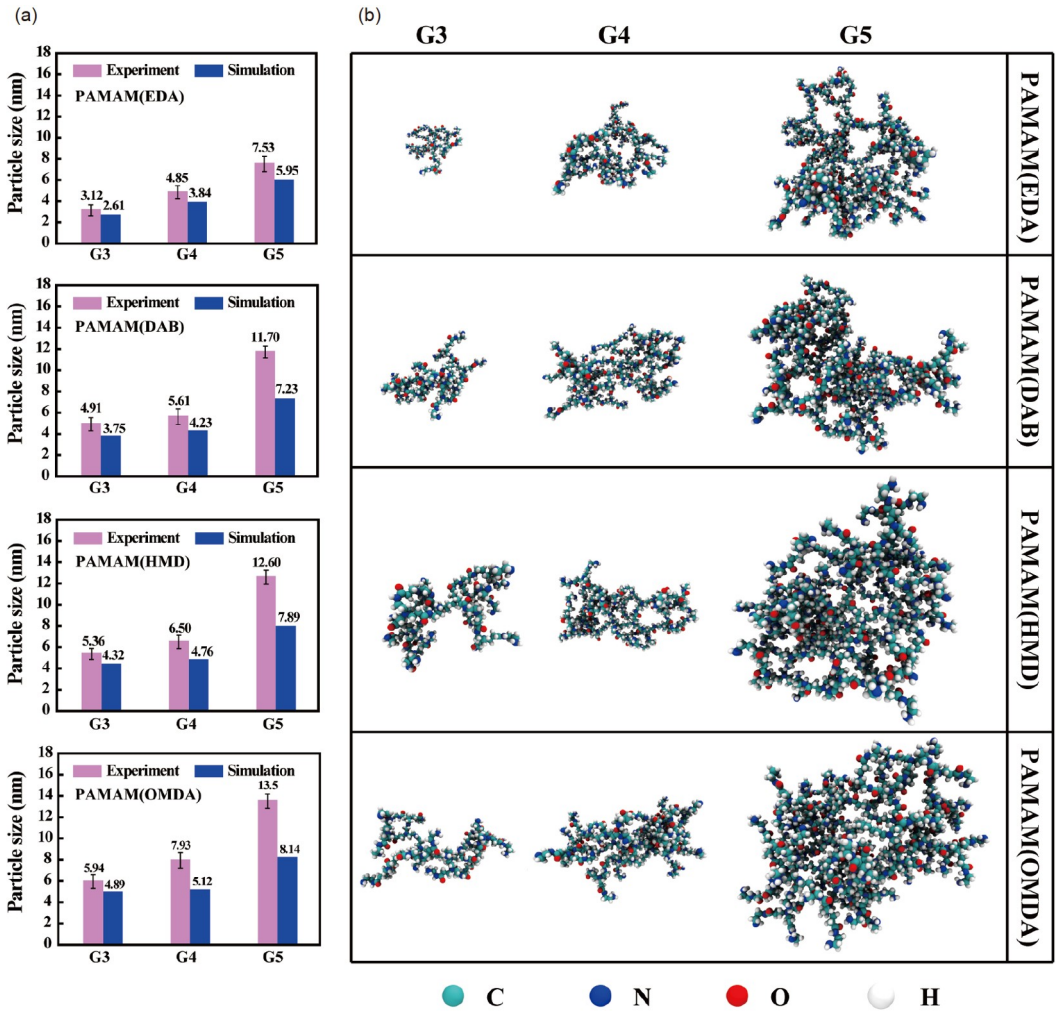

Figure 2 (Color online) (a) Particle size of dendrimers based on experiments and simulations; (b) equilibrium configuration of dendrimers in MD simulations.

sides, as the generation increases, entanglement and aggregation may appear between intermolecular chains, which also causes differences in results.

The equilibrium configuration of dendrimers in MD simulation was shown in Figure 2(b). From the third generation of molecules, the cavity with a large opening degree appears. With the increase of generation, the number and volume of cavities increase, while the opening degree of some cavities decreases. This result showed us that the particle size of dendrimers or drug-loaded complexes tested in aqueous solutions might differ from those designed in the protocol. In addition, external energy needs to be given to open the cavity during the drug loading process.

4.2 Drug loading

Three commonly used chemotherapeutic drugs (DOX, TAX, HCPT) are used as model drugs. As shown in Figure 3(a), the LC of different dendrimers for three drugs is not much different. The LC of PAMAM(EDA)@drugs and PAMAM (OMDA)@drugs is about 8.1%–8.8% and 8.6%–9.4%, respectively. As far as the same drug is concerned, the dendrimer with high generation exhibits higher drug loading (Table S4). The growth of the fatty amine chain also slightly increased the drug loading. Short aliphatic amines and low generations of dendrimers result in small cavities and large steric hindrances, which prevent drug molecules from interacting well with dendrimers. Many cavities are semi-open. Most drug molecules are not completely wrapped in the cavities of PAMAM. The small cavities are not significant for the actual drug loading after statistics. As can be seen from the characteristic snapshots in simulations (Figure 3(b)), the DOX/TAX/HCPT molecules can be trapped in the PAMAM dendrimers and stable dendrimer@drug complexes are formed. Some differences exist among the conformational structures of the different generation PAMAM dendrimers complexed with drug molecules. As for G3 dendrimer@drug complexes, drug molecules are inclined to associate with outer branches of PAMAM dendrimers, and the number of bound drug molecules is 1–2 for the G3

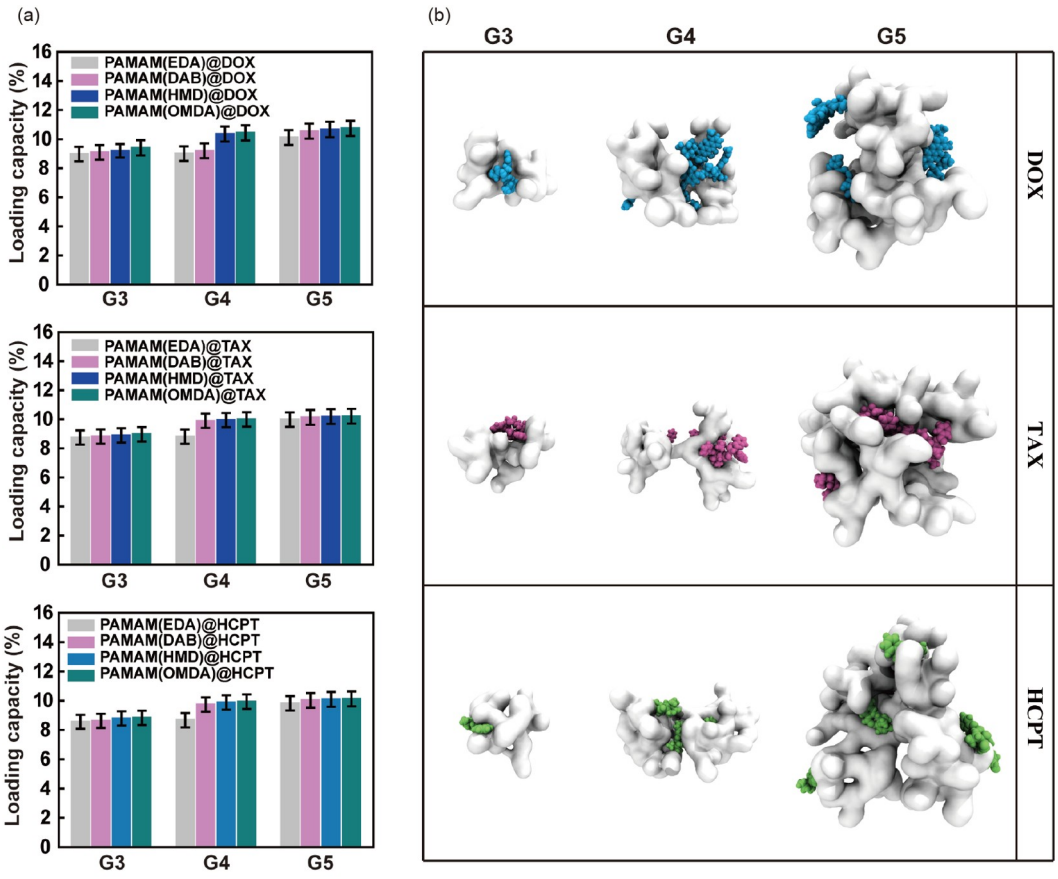

Figure 3 (Color online) (a) Loading capacity and (b) equilibrium configuration of various dendrimer@drug complexes.

dendrimer@drug complex. For G4 dendrimer@drug complexes, the number of bounded drug molecules increases to 3–5, and some drug molecules were found to be able to insert into the interior cavities of PAMAM dendrimers. For G5 dendrimer@drug complexes, due to the increase of interior cavities, internal encapsulation plays a more critical role in the complexation of drugs, and the number of bounded drug molecules is 4–6 for the G5 dendrimer@drug complex. The LC of PAMAM is closely related to the generation. It may be that the masses of dendrimers and drug molecules increase simultaneously, which results in the calculated LC change not being obvious.

4.2.1 Internal structure of PAMAM dendrimers

The structural properties of dendrimers are analyzed at the atomic level to investigate the mechanism of drug-loading behavior further. The planar density distributions of dendrimers were obtained along the *Z*-direction and with a grid size of 0.1 nm, as shown in Figure 4(a), which can help us to get insight into the internal structure of PAMAM. Previous studies have shown that uncharged PAMAM dendrimers with EDA as core possess a "dense core" structure with relatively flexible branches due to entropic contributions [31], which is consistent with the in-plane number density distribution of G3/4/5 PAMAM(EDA) in this study. But interestingly, it can be seen directly that the bright scope in planar density distribution gradually faded and the "dense core" structure gradually disappeared from PAMAM(EDA) to PAMAM(OMDA). The relatively loose internal structure leads to the increased molecular size of PAMAM dendrimers as stated above. Importantly, due to the steric effect and disturbance of the hydrocarbon chain, the density distributions of PAMAM dendrimers become more uniform as the aliphatic amine segment grows. Accordingly, an increasing number of interior cavities of PAMAM dendrimer can be utilized to carry drug molecules, therefore leading to the enhanced LC. To further quantify the variation of the internal structure of PAMAM dendrimers, the solvent-accessible surface area (SASA) was investigated, which can reflect the free volume within dendrimers that enables the encapsulation of drug molecules. As shown in Figure 4(b), the SASA of PAMAM is increased with the increasing generation and structural unit length. The variation trend of SASA confirms that the free interior volume of PAMAM dendrimers is enhanced by manipulating the aliphatic amines.

4.2.2 Intermolecular forces between dendrimers and drug molecules

To understand the impact of internal structure change on drug encapsulation, the non-covalent interactions between

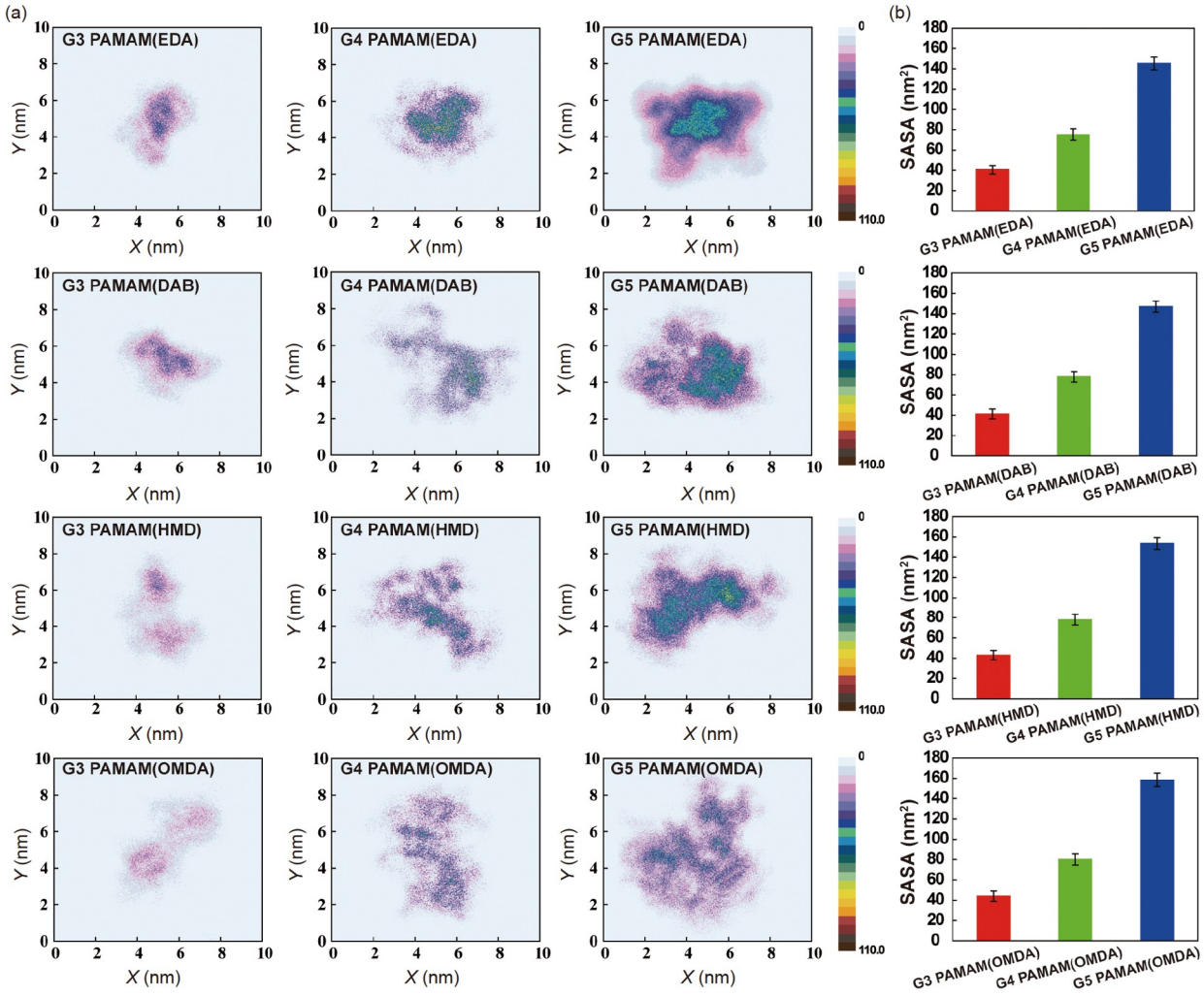

Figure 4 (Color online) (a) Planar density distribution of PAMAM dendrimers (*Z*-direction is perpendicular to the surface and the densities are expressed in the number of atoms/molecules nm^{-3}); (b) the solvent-accessible surface area (SASA) of PAMAM dendrimers.

PAMAM dendrimers and drug molecules are systematically analyzed. The simulation results illustrate that both the van der Waals (vdW) interaction and electrostatic interaction contribute to the formation of dendrimer@drug complexes. As shown in Figure 5(a) and (b), the vdW interaction is more pronounced. The vdW interaction and electrostatic interaction between PAMAM dendrimers and DOX/TAX/HCPT molecules are all enhanced as the length of the aliphatic amine increases. Many experimental studies indicate that the hydrogen bond interaction plays an important role in the encapsulation of drugs [32,33]. In this study, the hydrogen bonding between PAMAM dendrimers and drug molecules is also observed. The statistical analysis of hydrogen bonding illustrates that for dendrimers of the same generation, the longer the chain of aliphatic amine molecules of PAMAM dendrimers, the more hydrogen bonds formed with the drug molecules (Figure 5(c)). Representative snapshot of the hydrogen bonding between PAMAM dendrimer and TAX molecule is shown in Figure 5(d). We propose that the loose internal structure leads to the expansion of the internal cavity, thereby increasing the number of amine groups involved in the hydrogen bond formation in the PAMAM dendrimer (as demonstrated in the investigation of SASA).

Moreover, the number of amino groups on the periphery of high-generation dendrimers increases significantly, which is also conducive to forming hydrogen bonds. The molecular weight and structure of the drug molecule, as well as the number of polar groups in the molecule, will affect the interaction between the drug molecule and the dendrimer. The loading of drugs is determined by a variety of forces, and one of them may be dominant. It should also be noted that the LC is calculated based on the mass and cannot be simply compared based on the strength of the intermolecular forces. The simulation results show that long-chain fatty amines loosen the structure of PAMAM dendrimers, which helps increase the interaction between PAMAM dendrimers and drug molecules, thereby increasing the payload of PAMAM dendrimers. The experiment process will be affected by more

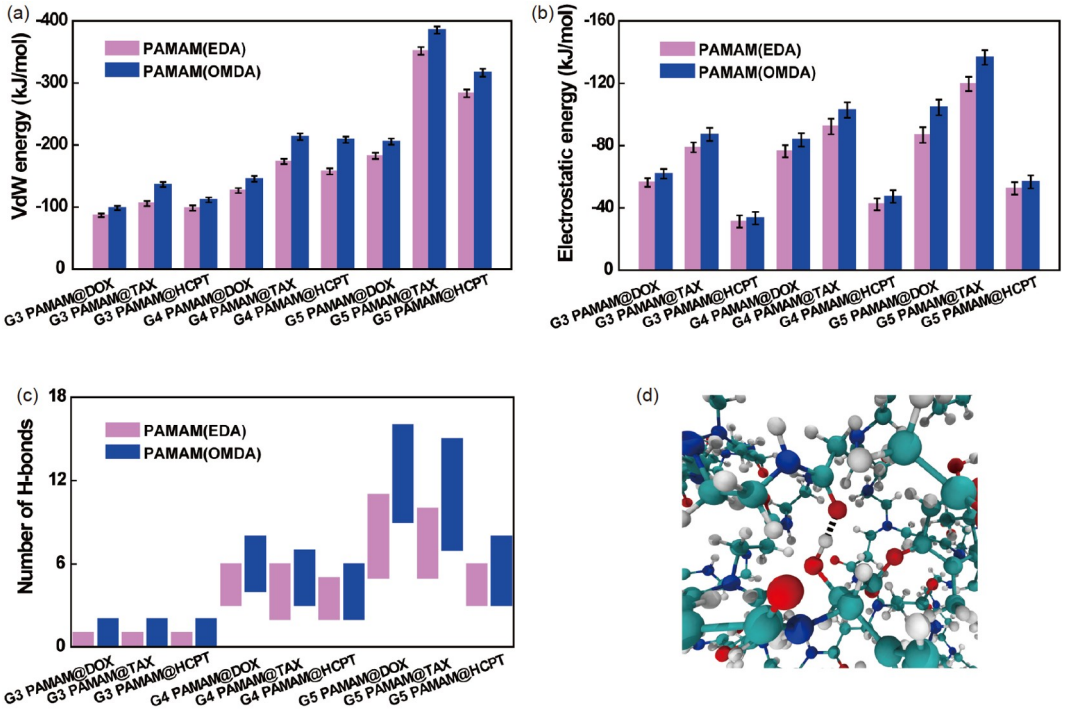

Figure 5 (Color online) (a) vdW interaction energy, (b) electrostatic interaction energy, and (c) the number of H-bonds between PAMAM(EDA)/PAMAM (OMDA) and drug molecules. (d) Representative snapshot of the hydrogen bonding between PAMAM dendrimer and TAX molecule.

factors, and the actual interaction between dendrimers and drug molecules in solution will be more complicated. The simulation results can be used to assist in guiding or explaining experimental phenomena.

4.3 Drugs release

In the process of carrier transportation, premature release of the drug is expected to be avoided. When the vectors reach the lesion site, the drug needs to be released effectively. Here, we discussed the escape of drug molecules from PAMAM dendrimers. The drug release of PAMAM@drug complexes performed at pH 7.4 is shown in Figure 6. After 15 h, the release reaches its maximum value of about 19%–25%.

4.4 Umbrella sampling simulation and binding energies

The binding energies between PAMAM dendrimers and drug molecules were studied using umbrella sampling simulation to elucidate the stability of PAMAM@drug complexes and the mechanism of drug release in different systems. The stable dendrimer-drug complexes were placed in a rectangular simulation box of 8 nm× 8 nm × 15 nm that contains 14000 methanol molecules. After energy minimization and MD simulation in the NPT ensemble, the COM of a selected drug molecule was pulled along the given reaction coordinate. At the same time, the PAMAM dendrimer was restrained, as shown in Figure 7. A series of frames were extracted from the trajectory, and each configuration corresponds to the desired COM spacing of less than 0.3 Å. Through a series of umbrella sampling simulations (5 ns for every sampling window), the binding energy between target molecules can be obtained from the PMF profile [34]. Separate simulations are run along the reaction coordinate ξ, biased by umbrella potentials $W_i(\xi)$, expressed as an equation:

$$W_i(\xi) = \frac{K_i}{2}(\xi - \xi_i^c)^2, \tag{3}$$

where ξ_i^c is the position at which the system is restrained with force constant K_i.

Here, the system of G5 OMDA PAMAM-TAX has been chosen as an example to validate the accuracy of umbrella sampling simulation. As illustrated in representative snapshots of the pulling process (Figure 7(a)), a selected TAX molecule was pulled along the given reaction coordinate, and the PMF vs. the distance between the COM of G5 OMDA PAMAM and TAX molecule is shown in Figure 7(b). According to the profile of PMF, the lowest energy configuration is at a distance of 1.2 nm, and the presence of potential well indicates that the TAX molecules tend to associate with PAMAM dendrimer to form the stable dendrimer-drug complex. With the increase of ξ, the values of PMF converge to a stable value. The binding energy obtained here corresponds to −11.82±0.92 kCal/mol. In addition, the statistical

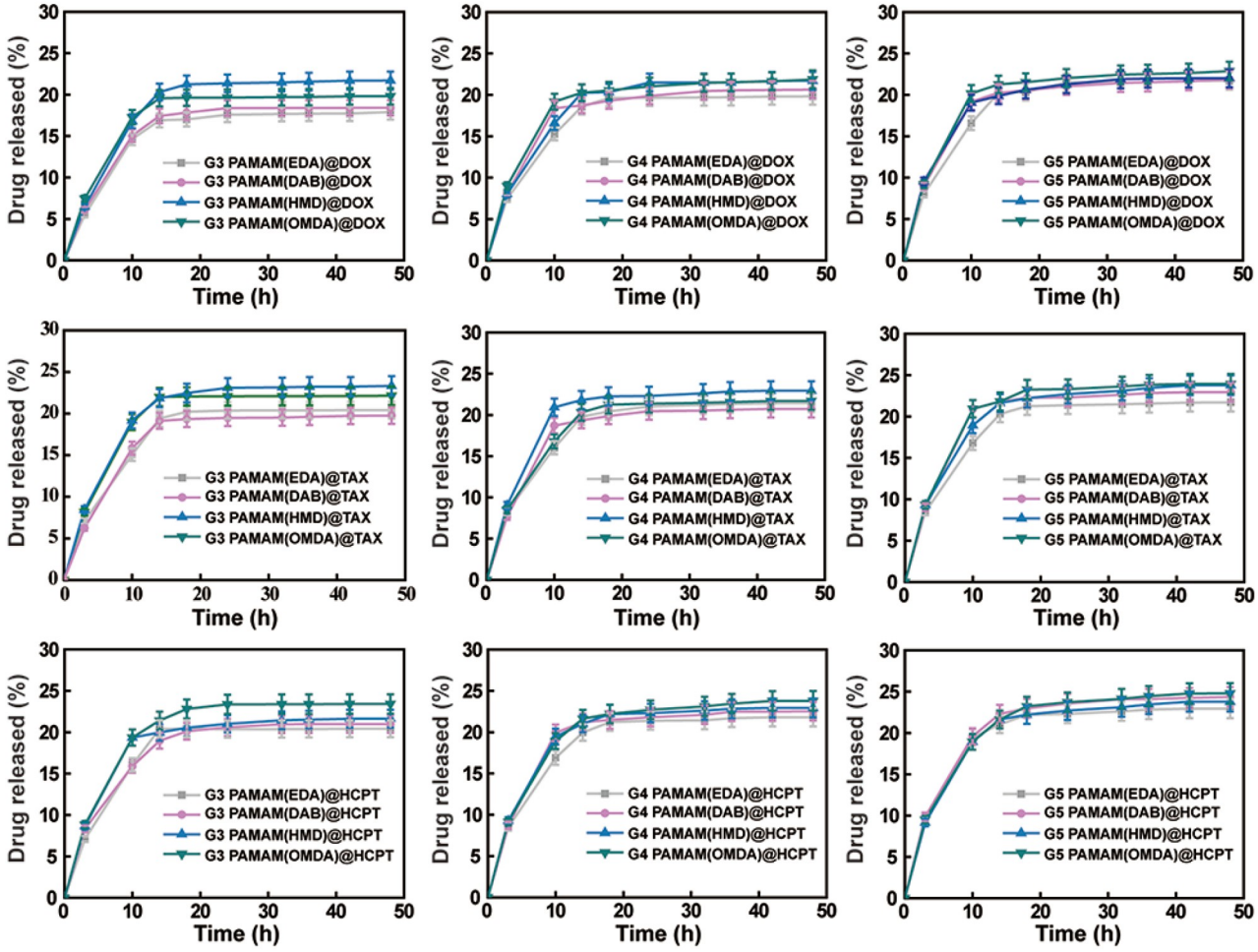

Figure 6 (Color online) Drug release behavior of PAMAM@drug complexes.

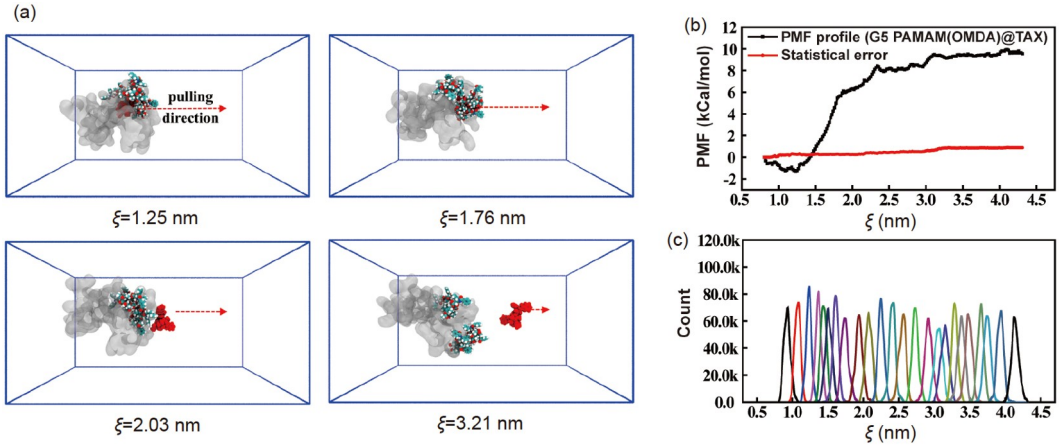

Figure 7 (Color online) (a) Representative snapshots of pulling simulation (G5 OMDA PAMAM-Tax molecule). (b) Potential of mean force profile and statistical error in umbrella sampling for G5 OMDA PAMAM-TAX and (c) the corresponding umbrella histograms.

error and corresponding umbrella histograms (Figure 7(c)) demonstrate that the sampling is adequate and the simulation result is reliable.

The binding energies between PAMAM dendrimers and drug molecules are summarized in Table 1. The negative value of binding energies implies that the DOX/TAX/HCPT molecules all tend to associate with PAMAM dendrimers to form dendrimer@drug complexes. According to the values of binding energies, the introduction of long-chain fatty amines can slightly promote the association between PA-

MAM dendrimers and drug molecules. As the generation of dendrimers increases, the binding energy rises, which indicates that drug molecules are less prone to disassociate with a high-generation of PAMAM dendrimers. In other words, the lower the binding energy, the easier it is for the dendrimer to load the drug, while the more difficult it is for the drug molecule to be released from the dendrimer. In addition, it is noteworthy that the environment can influence the release kinetics. Although it is still challenging to model intracellular and extracellular environments in MD simulations, with the development of the simulation method and computational resource, we believe that the model of dendrimer@drug complexes and their interaction with the biological interface can be closer to the real situation.

4.5 *In vitro* anti-tumor test

The cell viability of HepG2 and NIH 3T3 cells treated with PAMAM dendrimers (Figure 8(a)) and PAMAM@drug complexes (Figure 8(b)) was tested by MTT assay, respectively. HepG2 is an immortalized cell line consisting of human liver carcinoma cells, and NIH 3T3 is mouse embryonic fibroblast cells. As far as dendrimers are concerned, at high concentrations, G5 dendrimers exhibit the highest cytotoxicity at high concentrations, which is consistent with the previous report [3]. The amino groups on the surface of dendrimers are positive under physiological conditions, which is the main cause of cytotoxicity. At the same concentration, PAMAM(OMDA) exhibits the highest toxicity. This may be due to its soft and malleable molecules being easier to attach to cell membranes. Compared with PAMAM dendrimers, the dendrimer@drug complexes showed greater cytotoxicity. This is the result of the combined action of chemotherapeutic drugs and dendrimers. Generally, higher drug loading means more effective cell killing.

According to the above simulation results, it can be known that high-generation dendrimers can be loaded with more drugs and have more sites on their surface that can bind to drug molecules. Although the binding energy will affect the release of the drug, it may not be the main influencing factor based on the test results. Therefore, under the joint action of various factors, the trend of cell viability is consistent with popular perception. In addition, the dendrimer@drug complexes exhibited similar cytotoxicity both in tumor cell lines and normal cell lines. It can be seen that dendrimer-based drug carriers that have not undergone targeted modification have no ability to distinguish tumor cells from normal cells.

5 Conclusion

The relationship between PAMAM and several typical drug molecules, including equilibrium configuration and non-

Table 1 The binding energies between PAMAM dendrimers and drug molecules

Binding energy (kCal/mol)	PAMAM@DOX	PAMAM@TAX	PAMAM@HCPT
G3 PAMAM(EDA)	−2.42±0.66	−3.89±0.84	−3.43±0.80
G3 PAMAM(OMDA)	−2.53±0.59	−4.06±0.85	−3.46±0.81
G4 PAMAM(EDA)	−5.25±0.82	−7.37±0.97	−4.61±0.93
G4 PAMAM(OMDA)	−5.59±0.73	−7.93±0.94	−4.70±0.85
G5 PAMAM(EDA)	−9.02±1.01	−10.39±0.89	−7.96±0.90
G5 PAMAM(OMDA)	−9.74±0.94	−11.82±0.92	−8.13±0.88

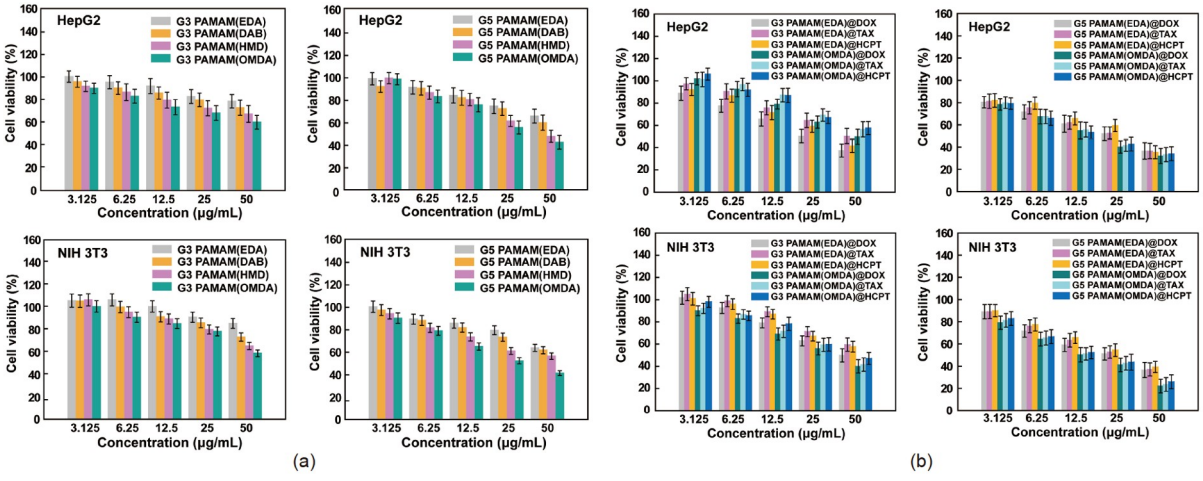

Figure 8 (Color online) The cell viability of HepG2 and NIH 3T3 cells treated with (a) PAMAM dendrimers and (b) PAMAM@drug complexes.

covalent interaction, has been studied. Utilizing all-atom molecular dynamic simulations has indicated that the structural units have a marked effect on the dendrimers' size and internal structure. As the molecular chain of the structural unit increases, the density distribution of PAMAM dendrimers turned to be more uniform. The variation of the internal structure of dendrimers can further lead to the increase of the non-covalent interaction between PAMAM dendrimers and drug molecules. The conclusion enriches the understanding of dendrimer drug delivery and can be used to assist in explaining the drug release behavior of PAMAM as a carrier. It also provides a theory for improving the delivery efficiency of dendrimers. Considering the cumbersome preparation process of dendrimers, it is necessary to choose a balance between biocompatibility, drug-loading capacity, and ease of preparation.

This work was supported by the National Natural Science Foundation of China (Grant Nos. 21874078, 22074072, and 22274083), the Taishan Young Scholar Program of Shandong Province (Grant No. tsqn20161027), the China Postdoctoral Science Foundation (Grant No. 2018M630752), the Postdoctoral Scientific Research Foundation of Qingdao, the Innovation and Development Joint Fund of Natural Science Foundation of Shandong Province (Grant No. ZR2022LZY022), the Science and Technology Planing Project of South District of Qingdao City (Grant No. 2022-4-005-YY), the Exploration Project of the State Key Laboratory of BioFibers and Eco-Textiles of Qingdao University (Grant No. TSKT202101), and the High Level Discipline Project of Shandong Province.

Supporting Information

The supporting information is available online at tech.scichina.com and link.springer.com. The supporting materials are published as submitted, without typesetting or editing. The responsibility for scientific accuracy and content remains entirely with the authors.

1 Lu Y, Slomberg D L, Shah A, et al. Nitric oxide-releasing amphiphilic poly(amidoamine) (PAMAM) dendrimers as antibacterial agents. Biomacromolecules, 2013, 14: 3589–3598
2 Zhou L, Shan Y, Hu H, et al. Synthesis and biomedical applications of dendrimers. Curr Org Chem, 2018, 22: 600–612
3 Cong H, Zhou L, Meng Q, et al. Preparation and evaluation of PAMAM dendrimer-based polymer gels physically cross-linked by hydrogen bonding. Biomater Sci, 2019, 7: 3918–3925
4 Maji S, Agarwal T, Maiti T K. PAMAM (generation 4) incorporated gelatin 3D matrix as an improved dermal substitute for skin tissue engineering. Colloids Surfs B-Biointerfaces, 2017, 155: 128–134
5 Luong D, Kesharwani P, Deshmukh R, et al. PEGylated PAMAM dendrimers: Enhancing efficacy and mitigating toxicity for effective anticancer drug and gene delivery. Acta Biomater, 2016, 43: 14–29
6 Sun Y, Ma X, Jing X, et al. PAMAM-functionalized cellulose nanocrystals with needle-like morphology for effective cancer treatment. Nanomaterials, 2021, 11: 1640
7 Sonuç Karaboğa M N, Sezgintürk M K. Determination of C-reactive protein by PAMAM decorated ITO based disposable biosensing system: A new immunosensor design from an old molecule. Talanta, 2018, 186: 162–168
8 Sun Y, Hu H, Jing X, et al. Co-delivery of chemotherapeutic drugs and cell cycle regulatory agents using nanocarriers for cancer therapy. Sci China Mater, 2021, 64: 1827–1848
9 Sun Y, Jing X, Ma X, et al. Versatile types of polysaccharide-based drug delivery systems: From strategic design to cancer therapy. Int J Mol Sci, 2020, 21: 9159
10 Sun Q, Sun X, Ma X, et al. Integration of nanoassembly functions for an effective delivery cascade for cancer drugs. Adv Mater, 2014, 26: 7615–7621
11 Xiong Z, Shen M, Shi X. Dendrimer-based strategies for cancer therapy: Recent advances and future perspectives. Sci China Mater, 2018, 61: 1387–1403
12 Zou W T, Zhong W, Sun M G, et al. pH-Responsive dendrimer-functionalized cotton cellulose nanocrystals for effective cancer treatment. Ferroelectrics, 2021, 578: 108–112
13 Wu J S, Li J X, Shu N, et al. A polyamidoamine (PAMAM) derivative dendrimer with high loading capacity of TLR7/8 agonist for improved cancer immunotherapy. Nano Res, 2022, 15: 510–518
14 Pishavar E, Oroojalian F, Salmasi Z, et al. Recent advances of dendrimer in targeted delivery of drugs and genes to stem cells as cellular vehicles. Biotechnol Prog, 2021, 37: e3174
15 Ren L, Lv J, Wang H, et al. A coordinative dendrimer achieves excellent efficiency in cytosolic protein and peptide delivery. Angew Chem Int Ed, 2020, 59: 4711–4719
16 Zhang C, Pan D, Luo K, et al. Dendrimer-doxorubicin conjugate as enzyme-sensitive and polymeric nanoscale drug delivery vehicle for ovarian cancer therapy. Polym Chem, 2014, 5: 5227–5235
17 Tian W, Ma Y. Theoretical and computational studies of dendrimers as delivery vectors. Chem Soc Rev, 2013, 42: 705–727
18 Sathe R Y, Bharatam P V. Drug-dendrimer complexes and conjugates: Detailed furtherance through theory and experiments. Adv Colloid Interface Sci, 2022, 303: 102639
19 Tian F, Lin X, Valle R P, et al. Poly(amidoamine) dendrimer as a respiratory nanocarrier: Insights from experiments and molecular dynamics simulations. Langmuir, 2019, 35: 5364–5371
20 Wang B, Sun Y, Davis T P, et al. Understanding effects of PAMAM dendrimer size and surface chemistry on serum protein binding with discrete molecular dynamics simulations. ACS Sustain Chem Eng, 2018, 6: 11704–11715
21 Liu Y, Bryantsev V S, Diallo M S, et al. PAMAM dendrimers undergo pH responsive conformational changes without swelling. J Am Chem Soc, 2009, 131: 2798–2799
22 Jafari M, Mehrnejad F, Talandashti R, et al. Effect of the lipid composition and cholesterol on the membrane selectivity of low generations PAMAM dendrimers: A molecular dynamics simulation study. Appl Surf Sci, 2021, 540: 148274
23 Maingi V, Kumar M V S, Maiti P K. PAMAM dendrimer-drug interactions: Effect of pH on the binding and release pattern. J Phys Chem B, 2012, 116: 4370–4376
24 Jain V, Maiti P K, Bharatam P V. Atomic level insights into realistic molecular models of dendrimer-drug complexes through MD simulations. J Chem Phys, 2016, 145: 124902
25 Jing X, Sun Y, Liu Y, et al. Alginate/chitosan-based hydrogel loaded with gene vectors to deliver polydeoxyribonucleotide for effective wound healing. Biomater Sci, 2021, 9: 5533–5541
26 Raemdonck K, Demeester J, de Smedt S. Advanced nanogel engineering for drug delivery. Soft Matter, 2009, 5: 707–715
27 Van Der Spoel D, Lindahl E, Hess B, et al. GROMACS: Fast, flexible, and free. J Comput Chem, 2005, 26: 1701–1718
28 Martínez L, Andrade R, Birgin E G, et al. PACKMOL: A package for building initial configurations for molecular dynamics simulations. J Comput Chem, 2009, 30: 2157–2164
29 Kästner J. Umbrella sampling. WIREs Comput Mol Sci, 2011, 1: 932–942
30 Gao W, Jiao Y, Dai L L. The effects of size, shape, and surface composition on the diffusive behaviors of nanoparticles at/across water-oil interfaces via molecular dynamics simulations. J Nanopart Res, 2016, 18: 91

31 Barra P A, Barraza L, Jiménez V A, et al. Complexation of mefenamic acid by low-generation PAMAM dendrimers: Insight from NMR spectroscopy studies and molecular dynamics simulations. Macromol Chem Phys, 2014, 215: 372–383
32 Hu J, Xu T, Cheng Y. NMR insights into dendrimer-based host-guest systems. Chem Rev, 2012, 112: 3856–3891
33 Meng Q, Hu H, Zhou L, et al. Logical design and application of prodrug platforms. Polym Chem, 2019, 10: 306–324
34 Marzinek J K, Bond P J, Lian G, et al. Free energy predictions of ligand binding to an α-helix using steered molecular dynamics and umbrella sampling simulations. J Chem Inf Model, 2014, 54: 2093–2104